International Journal of Earth, Energy and Environmental Sciences
ISSN: 2517-942X
Vol:9, No:6, 2015

Time/Temperature-Dependent Finite Element Model of Laminated Glass Beams

Alena Zemanová, Jan Zeman, Michal Šejnoha

Abstract—The polymer foil used for manufacturing of laminated glass members behaves in a viscoelastic manner with temperature dependance. This contribution aims at incorporating the time/temperature-dependent behavior of interlayer to our earlier elastic finite element model for laminated glass beams. The model is based on a refined beam theory: each layer behaves according to the finite-strain shear deformable formulation by Reissner and the adjacent layers are connected via the Lagrange multipliers ensuring the inter-layer compatibility of a laminated unit. The time/temperature-dependent behavior of the interlayer is accounted for by the generalized Maxwell model and by the time-temperature superposition principle due to the Williams, Landel, and Ferry. The resulting system is solved by the Newton method with consistent linearization and the viscoelastic response is determined incrementally by the exponential algorithm. By comparing the model predictions against available experimental data, we demonstrate that the proposed formulation is reliable and accurately reproduces the behavior of the laminated glass units.

Keywords—Laminated glass, finite element method, finite-strain Reissner model, Lagrange multipliers, generalized Maxwell model, Williams-Landel-Ferry equation, Newton method.

I. Introduction

LAMINATED glass units consist of multiple layers of glass bonded together with a polymer foil, e.g. made of polyvinyl butyral (PVB). Three facts are important to understand the mechanical behavior of laminated glass members:

1) the polymer foil exhibits a time/temperature-dependent response [1], [2],
2) the ratio between the shear modulus of glass and polymer foil typically exceeds three orders of magnitude [3], [4], and Fig. 1,
3) glass structures are very slender and can exhibit significant geometrically nonlinear behavior [5], [6].

Our recently developed finite element model of elastic laminated glass beams under finite strain [7], derived from a refined plate theory by Mau [8], assumes planar cross-sections of individual layers but not of the whole laminated glass unit and takes into account the geometrically nonlinear behavior. Note that geometric nonlinearity is not relevant for simply supported laminated glass beams, but its effects can be significant for statistically indeterminate laminated glass beams and for the majority of laminated glass plates (including the most common boundary conditions – all edges simply supported [9], [10]).

A. Zemanová, Jan Zeman, and Michal Šejnoha are with the Department of Mechanics, Faculty of Civil Engineering, Czech Technical University in Prague, Thákurova 7, 166 29 Prague 6, Czech Republic, e-mail: zemanova.alena@gmail.com

The last important ingredient not implemented in our model [7] is the time/temperature-dependent response of the polymer interlayer. It is worth noting that viscoelastic effects are often neglected in the design practice, because the full analysis requires additional constitutive parameters and advanced software tools, which are seldom available for practitioners. The developments presented in this contribution aim at providing the tools to achieve such a more accurate description.

II. Behavior of Interlayer

The viscoelastic response is highly influenced by the material used in the interlayer. The present description is sufficiently general to accommodate all currently used material variants, although only PVB interlayer is mentioned in this contribution.

The available experimental data indicate that PVB is a linearly viscoelastic and temperature-dependent material [3], [4], [11], [12]. The main engineering property relevant to the composite behavior of the units is the shear-stress versus shear-strain characteristics of the interlayer. The shear modulus of the PVB interlayer G is experimentally determined as a function of duration of loading and temperature, see Fig. 1.

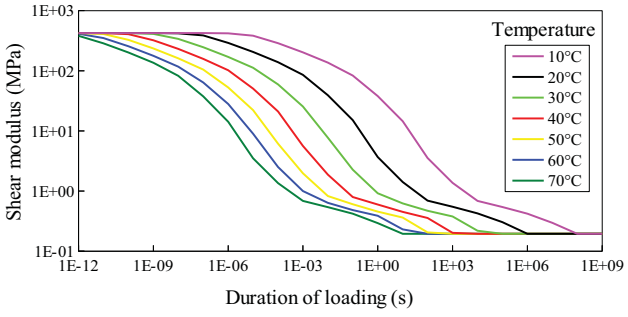

Fig. 1. Shear modulus G as a function of duration of loading and temperature, after [4].

III. Constitutive Relations

A. Assumptions

We start from an overview of constitutive relations for the polymer interlayer assuming that

1) under isothermal conditions, the material behaves as a linear elastic solid for volumetric loading and linear viscoelastic for deviatoric loading,

2) its deviatoric response can be accurately represented by the generalized Maxwell model,
3) the effect of temperature can be accounted for by the time-temperature superposition principle.

B. Volumetric-Deviatoric Split

In order to account for the different response to volumetric and deviatoric loads, we begin with a decomposition of the strain and stress tensors

$$\boldsymbol{\varepsilon}(t) = \frac{1}{3}\varepsilon_V(t)\boldsymbol{i} + \boldsymbol{e}(t), \tag{1a}$$

$$\boldsymbol{\sigma}(t) = \sigma_m(t)\boldsymbol{i} + \boldsymbol{s}(t), \tag{1b}$$

where t denotes the time instant, ε_m and σ_m are the mean strains and stresses, $\boldsymbol{e}$ and $\boldsymbol{s}$ refer to the deviatoric parts, and $\boldsymbol{i}$ is the unit tensor. Since the volumetric response is elastic, we have

$$\sigma_m(t) = K\left(\varepsilon_x(t) + \varepsilon_y(t) + \varepsilon_z(t)\right) = K\varepsilon_V(t), \tag{2}$$

where the bulk modulus K is assumed to be constant.

For a smooth strain history $\boldsymbol{e}(t)$ with $\boldsymbol{e}(0) = \boldsymbol{0}$, the deviatoric stress at time t reads, e.g [13, Section 1.2]

$$\boldsymbol{s}(t) = 2\int_0^t G(t')\frac{\mathrm{d}\boldsymbol{e}}{\mathrm{d}t'}(t')\,\mathrm{d}t', \tag{3}$$

where $G(t')$ denotes the shear relaxation modulus completely characterizing the response of the material.

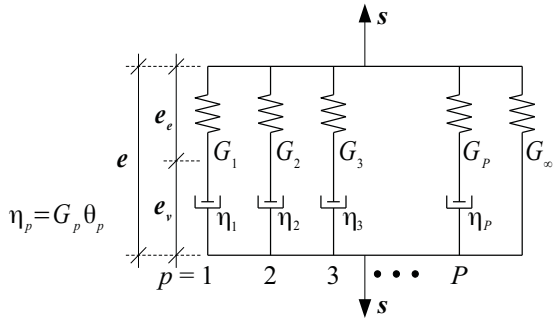

Fig. 2. Generalized Maxwell chain consisting of P viscoelastic units and elastic spring.

Under the second assumption, the shear relaxation modulus of the generalized Maxwell chain, Fig. 2, can be represented by the Dirichlet-Prony series [13, page 32]

$$G(t) = G_\infty + \sum_{p=1}^{P} G_p(\exp^{-\frac{t}{\theta_p}}) = G_0 - \sum_{p=1}^{P} G_p(1 - \exp^{-\frac{t}{\theta_p}}), \tag{4}$$

where the elastic shear modulus of the chain $G_0 = G_\infty + \sum_{p=1}^{P} G_p$, P is the number of viscoelastic units, G_p denotes the shear modulus of the p-th unit, $\theta_p = \eta_p/G_p$ is its relaxation time related to the viscosity η_p, and G_∞ is the shear modulus of the elastic spring.

C. Incorporation of Temperature Dependence

The temperature dependence is taken into account by the time-temperature superposition principle, in which the true time t is replaced by the effective value t/a_T adjusted by the temperature-dependent shift function a_T. We employ the Williams-Landel-Ferry (WLF) equation [14] for this purpose

$$\log a_T = -\frac{C_1(T - T_0)}{C_2 + T - T_0}, \tag{5}$$

where C_1 and C_2 are material constants, and T and T_0 are the current and reference temperatures, respectively.

D. Incremental Formulation at Material Point

The integral form of constitutive equations (3) is not very convenient for the numerical implementation, because all history variables during the whole loading process must be stored in order to evaluate the integral. Therefore, in the finite element implementation we will rely on the incremental approach, namely on the exponential algorithm [15].

To this purpose, we decompose the time interval of interest $\langle 0; t_{\max}\rangle$ into non-equidistant time instants $0 = t_0 < t_1 < t_2 < \cdots < t_{N-1} < t_N = t_{\max}$. The strain history over the time interval $\langle t_n; t_{n+1}\rangle$ is assumed to be known, so that

$$\boldsymbol{e}(t_{n+1}) = \boldsymbol{e}(t_n) + \Delta\boldsymbol{e}, \tag{6}$$

where $\Delta\boldsymbol{e}$ denotes the increment of deviatoric strain between the time instants t_n and t_{n+1}.[1] An analogous relation holds also for the deviatoric stresses

$$\boldsymbol{s}(t_{n+1}) = \boldsymbol{s}(t_n) + \Delta\boldsymbol{s}, \tag{7}$$

so that, assuming that the deviatoric stress at the beginning of the time step is known, the goal is to determine the corresponding increment of the deviatoric stress.

When the strain variation over the time interval of interest $\langle t_n; t_{n+1}\rangle$ is linear with respect to t, it is well-known that, e.g. [16, Chapter 10],

$$\Delta\boldsymbol{s} = 2\widehat{G}\Delta\boldsymbol{e} + \Delta\widehat{\boldsymbol{s}}, \tag{8}$$

where $\widehat{G}$ is the effective shear modulus over the time interval and $\Delta\widehat{\boldsymbol{s}}$ corresponds to the stress increment under the constant deformation due to relaxation effects. These quantities are provided by

$$\widehat{G} = G_\infty + \sum_{p=1}^{P} G_p\frac{a_T\theta_p}{\Delta t}(1 - \exp^{-\frac{\Delta t}{a_T\theta_p}}), \tag{9a}$$

$$\Delta\widehat{\boldsymbol{s}} = \sum_{p=1}^{P}\Delta\widehat{\boldsymbol{s}}_p = \sum_{p=1}^{P}\boldsymbol{s}_p(t_n)(\exp^{-\frac{\Delta t}{a_T\theta_p}} - 1). \tag{9b}$$

In (9), a_T abbreviates the value of the shift factor for a given time interval (we assume for simplicity that the temperature remains constant), and $\boldsymbol{s}_p$ and $\Delta\widehat{\boldsymbol{s}}_p$ stand for the values of the deviatoric stresses and its relaxation in the p-th unit of the generalized Maxwell chain. Finally, since the volumetric response is assumed to be elastic, we have

$$\Delta\sigma_m = K\Delta\varepsilon_V. \tag{10}$$

[1]Note that, in order to simplify the notation as much as possible, we omit the subscript related to the current time step for incremental variables.

IV. Incremental Viscoelasticity for Beam Theory

A. Incremental Formulation at Cross-Section

The relations (8)–(10) fully specify the incremental behavior for general three-dimensional stress and strain states. In order to derive the incremental constitutive equations for beams, we first recall that the only non-zero stress components are $\Delta\sigma_x$, consequently Δs_x, and $\Delta\tau_{xz} = \Delta s_{xz}$. We express the incremental formula of the internal forces at the cross-section level,

$$\Delta N_x(x) = \widehat{E}A\Delta\varepsilon_{x,0}(x) + \Delta\widehat{N}_x(x), \tag{11a}$$

$$\Delta M_y(x) = \widehat{E}I_y\Delta\kappa_y(x) + \Delta\widehat{M}_y(x), \tag{11b}$$

$$\Delta V_z(x) = k\widehat{G}A\Delta\gamma_{xz}(x) + \Delta\widehat{V}_z(x), \tag{11c}$$

where x specifies the position of the cross-section, $\Delta\varepsilon_{0,x}$ is the time increment of the centerline strain, $\Delta\kappa_y$ is the increment of the pseudo-curvature, A is the cross-section area, I_y the second moment of area, k the shear correction factor, and $\widehat{G}$ the effective shear modulus from (8). The effective Young modulus $\widehat{E}$ and the effective Poisson ratio $\widehat{\nu}$ are computed under the assumption of constant bulk modulus K. In (11), we utilized the fact that the effective material constants are the same for the whole layer, recall (9a).

We complement these relations with the update of history variables at the level of individual components of the Maxwell chain. In order to avoid excessive notation, we omit the dependence on x in the remainder of this section, as we implicitly assume that the derived relations hold for a given cross-section located at x. The increment of the normal stress for the p-th unit $\Delta s_{x,p}$ can be decomposed into a constant part and a part depending linearly on the position within a given cross-section z

$$\Delta s_{x,p}(z) = \Delta s^N_{x,p} + \Delta s^M_{x,p} z. \tag{12}$$

In analogy to (9b) we write

$$\Delta\widehat{s}^N_x = \sum_{p=1}^{P}\Delta\widehat{s}^N_{x,p} = \sum_{p=1}^{P} s^N_{x,p}(t_n)\left(\exp^{-\frac{\Delta t}{a_T\theta_p}} - 1\right), \tag{13a}$$

$$\Delta\widehat{s}^M_x = \sum_{p=1}^{P}\Delta\widehat{s}^M_{x,p} = \sum_{p=1}^{P} s^M_{x,p}(t_n)\left(\exp^{-\frac{\Delta t}{a_T\theta_p}} - 1\right), \tag{13b}$$

$$\Delta\widehat{\tau}_{xz} = \sum_{p=1}^{P}\Delta\widehat{\tau}_{xz,p} = \sum_{p=1}^{P}\tau_{xz,p}(t_n)\left(\exp^{-\frac{\Delta t}{a_T\theta_p}} - 1\right). \tag{13c}$$

These terms can be used to express the relaxation of the internal forces over the time increment, needed in (11), in the explicit form

$$\Delta\widehat{N}_x = (1+\widehat{\nu})A\Delta\widehat{s}^N_x, \tag{14a}$$

$$\Delta\widehat{M}_y = (1+\widehat{\nu})I_y\Delta\widehat{s}^M_x, \tag{14b}$$

$$\Delta\widehat{V}_z = kA\Delta\widehat{\tau}_{xz}. \tag{14c}$$

B. Solution Procedure

We extended the geometrically nonlinear solver from [7] to the incremental viscoelasticity formulation. The goal is to find the time increment of nodal displacements

$$\boldsymbol{r}(t_{n+1}) = \boldsymbol{r}(t_n) + \Delta\boldsymbol{r}, \tag{15}$$

but due to the geometrically nonlinear effects, the increment must be found by the Newton method. Assuming that the k-th iterate ${}^k\Delta\boldsymbol{r}$ is known, we express the $(k+1)$-th correction in the form

$${}^{k+1}\Delta\boldsymbol{r} = {}^k\Delta\boldsymbol{r} + {}^{k+1}\delta\boldsymbol{r}, \tag{16}$$

where ${}^{k+1}\delta\boldsymbol{r}$ and the vector of Lagrange multipliers ${}^{k+1}\boldsymbol{\lambda}$ are determined from the linearized system

$$\begin{bmatrix} {}^k\widehat{\boldsymbol{K}} & {}^k\boldsymbol{C}^{\mathsf{T}} \\ {}^k\boldsymbol{C} & \boldsymbol{0} \end{bmatrix}\begin{bmatrix} {}^{k+1}\delta\boldsymbol{r} \\ {}^{k+1}\boldsymbol{\lambda} \end{bmatrix} = -\begin{bmatrix} {}^k\widehat{\boldsymbol{f}}_{\mathrm{int}} - \boldsymbol{f}_{\mathrm{ext}}(t_{n+1}) + {}^k\Delta\widehat{\boldsymbol{f}}_{\mathrm{int}} \\ {}^k\boldsymbol{c} \end{bmatrix}. \tag{17}$$

The terms

$${}^k\widehat{\boldsymbol{K}} = \widehat{\boldsymbol{K}}_{\mathrm{t}}(\boldsymbol{r}(t_n) + {}^k\Delta\boldsymbol{r}) + \boldsymbol{K}_\lambda(\boldsymbol{r}(t_n) + {}^k\Delta\boldsymbol{r}, {}^k\boldsymbol{\lambda}), \tag{18a}$$

$${}^k\boldsymbol{C} = \nabla\boldsymbol{c}(\boldsymbol{r}(t_n) + {}^k\Delta\boldsymbol{r}), \tag{18b}$$

$${}^k\widehat{\boldsymbol{f}}_{\mathrm{int}} = \widehat{\boldsymbol{f}}_{\mathrm{int}}(\boldsymbol{r}(t_n) + {}^k\Delta\boldsymbol{r}), \tag{18c}$$

$${}^k\boldsymbol{c} = \boldsymbol{c}(\boldsymbol{r}(t_n) + {}^k\Delta\boldsymbol{r}), \tag{18d}$$

follow directly from the relations derived in [7]; the notation $\widehat{\boldsymbol{K}}_{\mathrm{t}}$ and $\widehat{\boldsymbol{f}}_{\mathrm{int}}$ is used to emphasize that these quantities are determined using the effective parameters $\widehat{G}$ and $\widehat{E}$. In addition, we have to account for the additional nodal forces arising from the relaxation effects

$${}^k\Delta\widehat{\boldsymbol{f}}_{\mathrm{int}} = \Delta\widehat{\boldsymbol{f}}_{\mathrm{int}}(\boldsymbol{r}(t_n) + {}^k\Delta\boldsymbol{r}). \tag{19}$$

These are obtained by the assembly of the element contributions

$$\Delta\widehat{\boldsymbol{f}}_{\mathrm{int},e}(\boldsymbol{r}_e) = \Delta\widehat{\boldsymbol{f}}^N_{\mathrm{int},e}(\boldsymbol{r}_e) + \Delta\widehat{\boldsymbol{f}}^V_{\mathrm{int},e}(\boldsymbol{r}_e) + \Delta\widehat{\boldsymbol{f}}^M_{\mathrm{int},e}(\boldsymbol{r}_e), \tag{20}$$

where the individual components are evaluated from the stress increments under the constant deformation due to relaxation effects (13), see [17, Section 6.3].

Finally, we summarize the one-step problem for the geometrically nonlinear formulation in Algorithm 1. The termination criteria for the iterative algorithm are set according to the two residuals, cf. [7],

$${}^k\eta_1 = \frac{\|{}^k\widehat{\boldsymbol{f}}_{\mathrm{int}} + {}^k\Delta\widehat{\boldsymbol{f}}_{\mathrm{int}} - \boldsymbol{f}_{\mathrm{ext}}(t_{n+1}) + {}^k\boldsymbol{C}^{\mathsf{T}}{}^k\boldsymbol{\lambda}\|_2}{\max\left(\|\boldsymbol{f}_{\mathrm{ext}}(t_{n+1})\|_2, 1\right)}, \tag{21}$$

$${}^k\eta_2 = \frac{\|{}^k\boldsymbol{c}\|_2}{\min_i h^{(i)}}, \tag{22}$$

where $h^{(i)}$ stands for thicknesses of individual layers with $i = 1, 2, 3$.

V. Validation of Model with Viscoelastic Behavior of Interlayer

Experimental data for the validation of the finite element model are reproduced from [18] and [4]. The mechanical properties of glass were determined from a static bending test, yielding the Young modulus $E = 72$ GPa and the Poisson ratio $\nu = 0.23$. The experimental viscoelastic characterization of PVB was made by subjecting specimens of thickness

Algorithm 1: Conceptual implementation of one-step exponential algorithm for geometrically nonlinear laminated beams

Data: load $\boldsymbol{f}_{\text{ext}}(t_{n+1})$, displacements $\boldsymbol{r}(t_n)$, and deviatoric stresses $[s^N_{x,p,e}, s^M_{x,p,e}, \tau_{xz,p,e}]^{n^e,P}_{e=1,p=1}$ at t_n, and tolerances ϵ_1 and ϵ_2

Result: displacements $\boldsymbol{r}(t_{n+1})$, deviatoric stresses $[s^N_{x,p,e}, s^M_{x,p,e}, \tau_{xz,p,e}]^{n^e,P}_{e=1,p=1}$

$k \leftarrow 0, {}^0\boldsymbol{\lambda} \leftarrow \boldsymbol{0}, {}^0\Delta\boldsymbol{r} \leftarrow \boldsymbol{0}$

assemble ${}^k\widehat{\boldsymbol{f}}_{\text{int}}$, ${}^k\Delta\widehat{\boldsymbol{f}}_{\text{int}}$, ${}^k\boldsymbol{c}$, and ${}^k\boldsymbol{C}$ from (18) and (19)

while $({}^k\eta_1 > \epsilon_1)$ *or* $({}^k\eta_2 > \epsilon_2)$ **do**

  assemble ${}^k\widehat{\boldsymbol{K}}$

  solve for $({}^{k+1}\delta\boldsymbol{r}, {}^{k+1}\boldsymbol{\lambda})$ from (17)

  ${}^{k+1}\Delta\boldsymbol{r} \leftarrow {}^k\Delta\boldsymbol{r} + {}^{k+1}\delta\boldsymbol{r}$

  assemble ${}^{k+1}\widehat{\boldsymbol{f}}_{\text{int}}$, ${}^{k+1}\Delta\widehat{\boldsymbol{f}}_{\text{int}}$, ${}^{k+1}\boldsymbol{c}$, and ${}^{k+1}\boldsymbol{C}$ from (18) and (19)

  $k \leftarrow k+1$

$\boldsymbol{r}(t_{n+1}) \leftarrow \boldsymbol{r}(t_n) + {}^{k+1}\Delta\boldsymbol{r}$

update

$$s^N_{x,p,e} \leftarrow s^N_{x,p,e} + \Delta s^N_{x,p,e}$$
$$s^M_{x,p,e} \leftarrow s^M_{x,p,e} + \Delta s^M_{x,p,e}$$
$$\tau_{xz,p,e} \leftarrow \tau_{xz,p,e} + \Delta\tau_{xz,p,e}$$

with $e = 1, 2, \ldots, n^e$ and $p = 1, 2, \ldots, P$

0.38 mm to tensile relaxation tests with the duration of 10 min. The PVB was tested at different temperatures from -15 °C to 50 °C in order to apply the time-temperature-superposition principle for construction of the PVB master curve. The resulting material constants of the generalized Maxwell chain, as provided in [4], are summarized in Table I, and the parameters of the Williams-Landel-Ferry (WLF) equation (5) are set to $C_1 = 12.6$, $C_2 = 74.46$, and $T_0 = 20$ °C. The bulk modulus of the interlayer is considered as $K = 2$ GPa.

TABLE I
GENERALIZED MAXWELL SERIES DESCRIPTION OF THE SHEAR RELAXATION MODULUS FOR PVB (AFTER [4]), $G_\infty = 1.9454\times10^{-4}$ GPA

p	θ_p [s]	G_p [GPa]
1	2.3660×10^{-7}	9.9482×10^{-2}
2	2.2643×10^{-6}	9.0802×10^{-2}
3	2.1667×10^{-5}	7.4140×10^{-2}
4	2.0733×10^{-4}	5.0772×10^{-2}
5	1.9839×10^{-3}	5.7856×10^{-2}
6	1.8984×10^{-2}	2.9055×10^{-2}
7	1.8165×10^{-1}	1.7601×10^{-2}
8	1.7382×10^{0}	3.0802×10^{-3}
9	1.6633×10^{1}	1.2001×10^{-3}
10	1.5916×10^{2}	1.1523×10^{-4}
11	1.5230×10^{3}	1.8237×10^{-4}
12	1.4573×10^{4}	4.1645×10^{-5}
13	1.3945×10^{5}	2.2405×10^{-4}

Several experimental tests were carried out in [18] for four types of laminated glass beams under uniform distributed loading. Seven concentrated loads were used to reproduce such loading conditions and the deflections at the mid-span were measured using a laser sensor. These experimental data are utilized here to validate the finite element model for laminated glass beams.

The reported results correspond to the discretization of the structure with 50 elements per layer for the beam. As for the loading history, it was parametrized by the relative magnitude function

$$m(t) = \begin{cases} 10^5 t & \text{for } t \le 10^{-5}\text{s}, \\ 1 & \text{otherwise}, \end{cases} \tag{23}$$

simulating a rapid loading reported in [4]. The time steps in the incremental algorithms were distributed uniformly in the logarithmic scale, in particular 6 time steps were used to discretize the interval $\langle 10^{-6}; 10^{-5}\rangle$, whereas the interval $\langle 10^{-5}; 10^{5}\rangle$ was decomposed into 24 time steps.

In Fig. 3–6, we present the experimental values of deflection together with the prediction of the proposed beam model with viscoelastic behavior of the interlayer. These data are

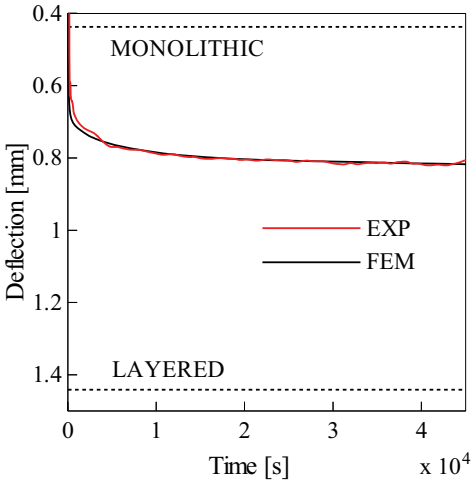

Fig. 3. Comparison of maximum deflections of a simply supported beam with a non-symmetric layout of layers with thicknesses glass layers 4 mm and 8 mm and PVB layer 0.38 mm, the length of 1 m, and the width of 0.1 m, under the uniform distributed loading of intensity $f_z = 38.25$ N/m at the temperature $T = 17.4$ °C. (EXP: experimental data, FEM: response of finite element model of laminated glass beam in terms of deflections.)

complemented with the values of deflections corresponding to the linear monolithic (with thickness equal to the combined thickness of glass layers) and layered (an assembly of independent glass layers) simply-supported beams under the constant load, in order to provide the upper and lower bounds.

The results confirm that the viscoelastic models of laminated glass beams reproduce the experimental data reasonably well with an error under approximately 7% in the central deflection (Fig. 3–5) and under 10% in the deflection at the mid-point of one of the spans (Fig. 6). Such an accuracy is consistent with the results of the static test reported in [7]. We attribute this difference mainly to the temperature variation during the experiment, since it follows from the WLF equation that the interlayer material is highly sensitive to temperature changes, and the only information about the temperature is its mean value during the experiment.

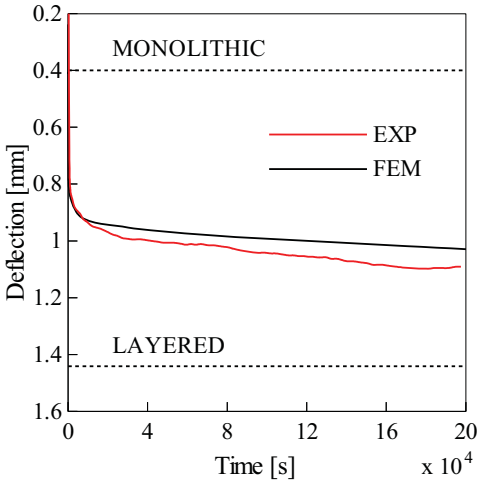

Fig. 4. Comparison of maximum deflections of a simply supported beam with a non-symmetric layout of layers with thicknesses of glass layers 4 mm and 8 mm and PVB layer 0.76 mm, the length of 1 m, and the width $b = 0.1$ m, under the uniform distributed loading of intensity $f_z = 38.25$ N/m at the temperature $T = 18.3\,^{\circ}$C.(EXP: experimental data, FEM: response of finite element model of laminated glass beam in terms of deflections.)

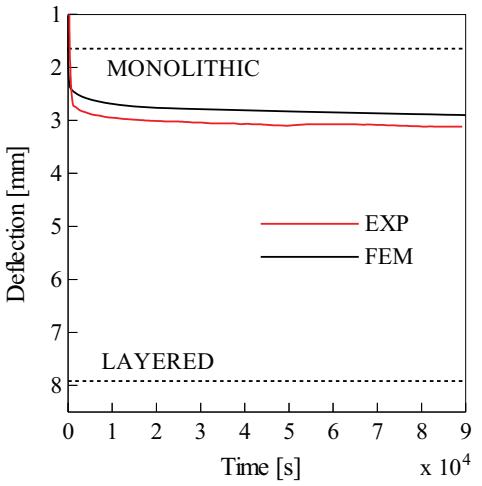

Fig. 5. Comparison of maximum deflections of a simply supported beam with a symmetric layout of layers with thicknesses of glass layers 3 mm and PVB layer 0.38 mm, the total length of 1 m, and the width of 0.1 m, under the uniform distributed loading of intensity $f_z = 19.7$ N/m at the temperature $T = 17.5\,^{\circ}$C. (EXP: experimental data, FEM: response of finite element model of laminated glass beam in terms of deflections.)

It is also worth noting that both the upper and lower bounds display significantly larger errors in deflections, which renders their prediction unsafe (monolithic bound) or uneconomical (layered bound).

VI. Parametric Study on Viscoelastic Behavior of Interlayer

The validation of the viscoelastic finite element models was performed in the previous section for statically determinate units that exhibit a negligible difference between the geometrically linear and nonlinear response. Therefore, the

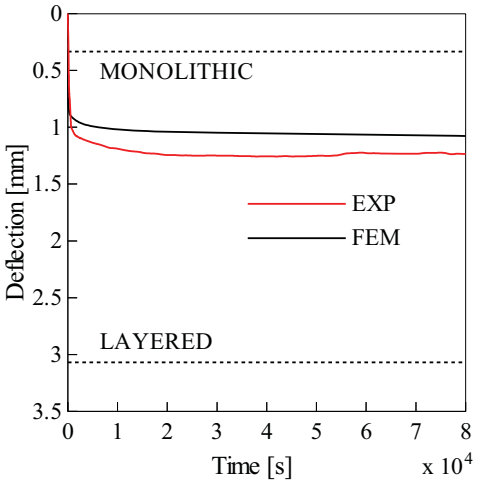

Fig. 6. Comparison of deflection at the mid-point of one of the spans of a two-span simply supported beam with a symmetric layout of layers with thicknesses of glass layers 4 mm and PVB layer 0.38 mm, length of 1.4 m, the spans of 0.7 m, and the width of 0.1 m, under the uniform distributed loading of intensity $f_z = 94.22$ N/m at the temperature $T = 17.8\,^{\circ}$C. (EXP: experimental data, FEM: response of finite element model of laminated glass beam in terms of deflections.)

purpose of the present section is to complement these results with a study on structures for which the effect of geometric nonlinearity is significant. Attention is also paid to the effect of temperature variation, accounted for by the Williams–Landel–Ferry formula (5). The material parameters for glass layers and PVB interlayer are set in the same way as in Section V, and so is the loading history, recall (23).

A laminated glass beam with both ends fixed is presented. The structure was subjected to a distributed load with the peak intensity $f_z = 10$ Nm^{-1} (so that the maximum deflections remain below $3,000/250 = 12$ mm in the nonlinear case), and was discretized with 50 elements per layer. Response of the structures is investigated for three constant temperatures $0\,^{\circ}$C, $25\,^{\circ}$C, and $50\,^{\circ}$C. The resulting evolution of the central deflection with time is plotted in Fig. 7–8 for both linear and nonlinear models. In addition to the standard upper and lower bounds, provided by the geometrically linear monolithic and layered approximations, we also provided the elastic response corresponding to the interlayer shear modulus set to the maximum elastic value G_0 and the long-term limit G_∞, recall (4).

The results are in full agreement with the outcomes presented in [1], namely that the laminated units exposed to temperatures around $0\,^{\circ}$C effectively behave as the monolithic ones, which also holds when the elastic shear modulus is used. For temperatures exceeding $50\,^{\circ}$C, the response almost immediately reaches the limit set by G_∞, but this value is still sufficient to ensure the interaction of the glass layers. For the intermediate temperatures, corresponding to room conditions, the viscoelastic effects become relevant, and the deflections interpolate the G_0–G_∞ bounds. It is interesting to note that these bounds are too far apart in the linear case (the relative difference in deflections is 135%), but for the geometrically

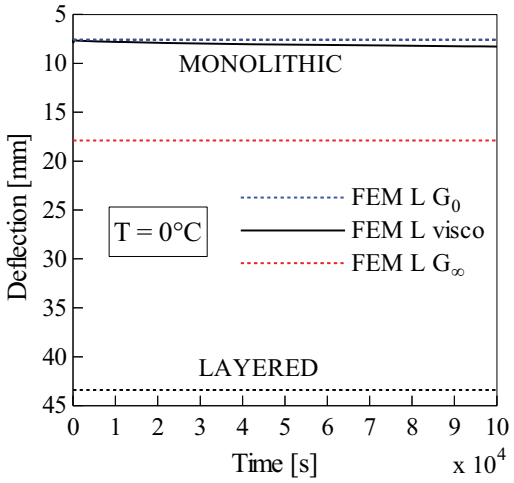

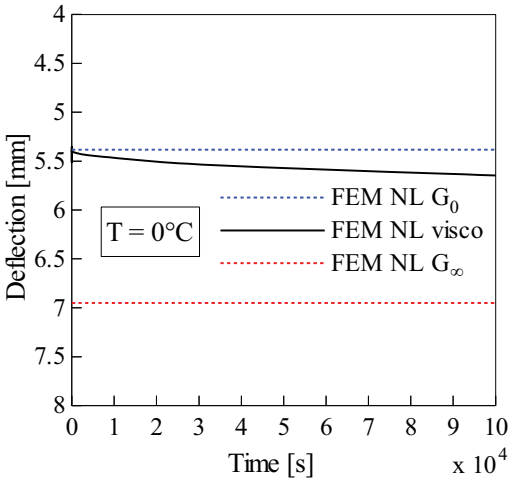

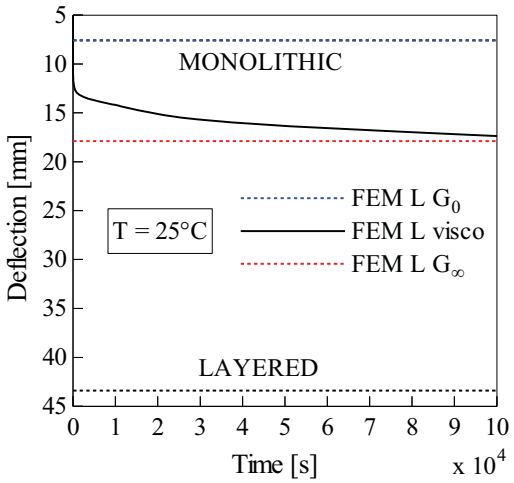

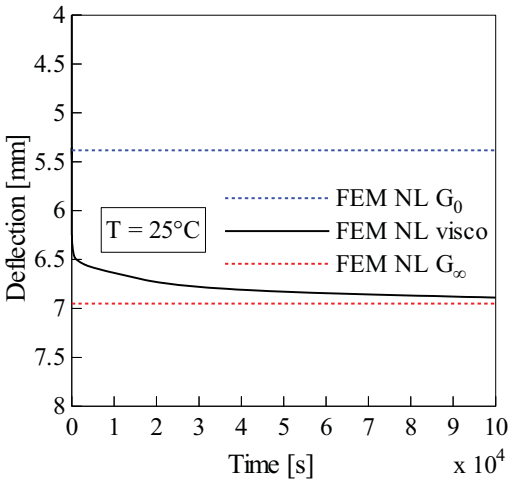

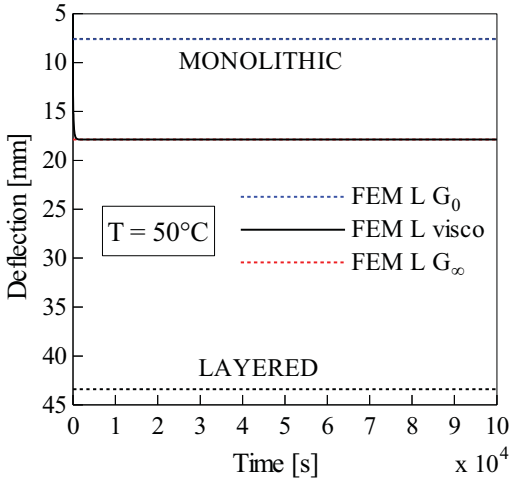

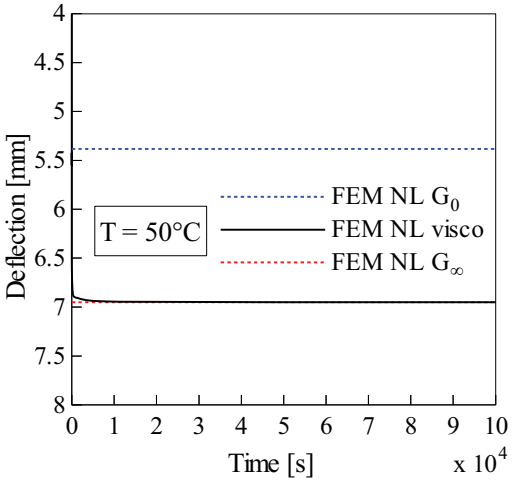

Fig. 7. Central deflections of a fixed-end beam with a symmetric layout of layers with thicknesses of glass layers 3 mm and PVB layer 0.76 mm, the length of 3 m, and width of 0.15 m, under the uniform distributed loading of intensity $f_z = 10$ N/m at the temperature $T = 0\,^{\circ}$C, $25\,^{\circ}$C, and $50\,^{\circ}$C. (FEM L: response of geometrically linear finite element model of laminated glass beam in terms of deflections.)

Fig. 8. Central deflections of a fixed-end beam with a symmetric layout of layers with thicknesses of glass layers 3 mm and PVB layer 0.76 mm, the length of 3 m, and width of 0.15 m, under the uniform distributed loading of intensity $f_z = 10$ N/m at the temperature $T = 0\,^{\circ}$C, $25\,^{\circ}$C, and $50\,^{\circ}$C. (FEM NL: response of geometrically nonlinear finite element model of laminated glass beam in terms of deflections.)

nonlinear model the difference remains below 30%.

VII. Conclusion

In conclusion, we conjecture on the basis of the performed validation and parametric study that:

1) The viscoelastic finite element model of laminated glass beams reproduces the experimental data reasonably well.
2) Both upper and lower bounds display significantly larger errors in deflections, which renders their prediction unsafe (monolithic bound) or uneconomical (layered bound).
3) The findings of parametric study highlight the need for geometrically nonlinear analyzes of laminated glass structures, in view of their rational design.

Acknowledgment

This contribution was supported by the European social fund within the framework of realizing the project "Support of inter-sectoral mobility and quality enhancement of research teams at Czech Technical University in Prague", CZ.1.07/2.3.00/30.0034. Period of the project's realization 1.12.2012 – 30.6.2015.

References

[1] R. A. Behr, J. E. Minor, and H. S. Norville, "Structural behavior of architectural laminated glass," *Journal of Structural Engineering*, vol. 119, no. 1, pp. 202–222, 1993.
[2] T. Serafinavičiusa, J. Lebeta, C. Loutera, T. Lenkimasc, and A. Kuranovasb, "Long-term laminated glass four point bending test with PVB, EVA and SG interlayers at different temperatures," *Procedia Engineering*, vol. 57, pp. 996–1004, 2013.
[3] S. J. Bennison, A. Jagota, and C. A. Smith, "Fracture of Glass/Poly(vinyl butyral) (Butacite®) laminates in biaxial flexure," *Journal of the American Ceramic Society*, vol. 82, no. 7, pp. 1761–1770, 1999.
[4] F. Pelayo, M. López-Aenlle, L. Hermans, and A. Fraile, "Modal scaling of a laminated glass plate," *5th International Operational Modal Analysis Conference*, pp. 1–10, 2013.
[5] C. V. G. Vallabhan, Y. C. Das, M. Magdi, M. Asik, and J. R. Bailey, "Analysis of laminated glass units," *Journal of Structural Engineering*, vol. 119, no. 5, pp. 1572–1585, 1993.
[6] A. V. Duser, A. Jagota, and S. J. Bennison, "Analysis of glass/polyvinyl butyral laminates subjected to uniform pressure," *Journal of Engineering Mechanics*, vol. 125, no. 4, pp. 435–442, 1999.
[7] A. Zemanová, J. Zeman, and M. Šejnoha, "Numerical model of elastic laminated glass beams under finite strain," *Archives of Civil and Mechanical Engineering*, vol. 14, no. 4, pp. 734–744, 2014.
[8] S. T. Mau, "A refined laminated plate theory," *Journal of Applied Mechanics–Transactions of the ASME*, vol. 40, no. 2, pp. 606–607, 1973.
[9] M. Z. Aşık and S. Tezcan, "A mathematical model for the behavior of laminated glass beams," *Computers & Structures*, vol. 83, no. 21–22, pp. 1742–1753, 2005.
[10] M. Z. Aşık, "Laminated glass plates: revealing of nonlinear behavior," *Computers & Structures*, vol. 81, no. 28–29, pp. 2659–2671, 2003.
[11] C. V. G. Vallabhan, Y. C. Das, and M. Ramasamudra, "Properties of PVB interlayer used in laminated glass," *Journal of Materials in Civil Engineering*, vol. 4, no. 1, pp. 71–76, 1992.
[12] A. K. Dhaliwal and J. N. Hay, "The characterization of polyvinyl butyral by thermal analysis," *Thermochimica Acta*, vol. 391, no. 1-2, pp. 245–255, 2002.
[13] R. Christensen, *Theory of Viscoelasticity: An Introduction*, 2nd ed. Elsevier, 1982.
[14] M. Williams, R. Landel, and J. Ferry, "The temperature dependence of relaxation mechanisms in amorphous polymers and other glass-forming liquids," *Journal of the American Chemical Society*, vol. 77, no. 14, pp. 3701–3707, 1955.
[15] O. C. Zienkiewicz, M. Watson, and I. P. King, "A numerical method of visco-elastic stress analysis," *International Journal of Mechanical Sciences*, vol. 10, no. 10, pp. 807–827, 1968.
[16] J. C. Simo and T. J. R. Hughes, *Computational Inelasticity*. Springer, 1998.
[17] A. Zemanová, "Numerical modeling of laminated glass structures," Ph.D. dissertation, Faculty of Civil Engineering, CTU, Prague, 2014.
[18] M. López-Aenlle, F. Pelayo, A. Fernández-Canteli, and M. A. García Prieto, "The effective-thickness concept in laminated-glass elements under static loading," *Engineering Structures*, vol. 56, pp. 1092–1102, 2013.

Alena Zemanová is a postdoctoral researcher at the Department of Mechanics, Faculty of Civil Engineering, Czech Technical University in Prague. Her research activities lie within numerical homogenization of plate structures and numerical modeling of laminated structures. E-mail: zemanova.alena@gmail.com.

Jan Zeman is an Associate Professor at the Department of Mechanics, Faculty of Civil Engineering, Czech Technical University in Prague. His research activities lie within analysis of heterogeneous materials and structures and applied mathematical modeling in engineering sciences.

Michal Šejnoha is a Full Professor at the Department of Mechanics, Faculty of Civil Engineering, Czech Technical University in Prague. His research interests lie within the analysis of heterogeneous materials and structures and computational geomechanics.